NASA TECHNICAL MEMORANDUM

NASA TM X-52788

NASA TM X-52788

THE EFFECT OF INLET TEMPERATURE DISTORTION ON THE PERFORMANCE OF A TURBO-FAN ENGINE COMPRESSOR SYSTEM

by Richard A. Rudey and Robert J. Antl
Lewis Research Center
Cleveland, Ohio

TECHNICAL PAPER proposed for presentation at
Sixth Propulsion Joint Specialists Conference sponsored by
the American Institute of Aeronautics and Astronautics
San Diego, California, June 22-26, 1970

THE EFFECT OF INLET TEMPERATURE DISTORTION ON THE PERFORMANCE OF A TURBO-FAN ENGINE COMPRESSOR SYSTEM

by Richard A. Rudey and Robert J. Antl

Lewis Research Center
Cleveland, Ohio

TECHNICAL PAPER proposed for presentation at

Sixth Propulsion Joint Specialists Conference sponsored by
the American Institute of Aeronautics and Astronautics
San Diego, California, June 22-26, 1970

NATIONAL AERONAUTICS AND SPACE ADMINISTRATION

THE EFFECT OF INLET TEMPERATURE DISTORTION ON THE PERFORMANCE OF A TURBO-FAN ENGINE COMPRESSOR SYSTEM

Richard A. Rudey and Robert J. Antl

Lewis Research Center
National Aeronautics and Space Administration
Cleveland, Ohio

Abstract

A turbo-fan engine was experimentally subjected to spatial and time-dependent inlet temperature distortions in an altitude test facility. A gaseous hydrogen fueled burner was used to produce the distortions. The purpose of the test was to determine the effect of circumferential extent, magnitude, and rate-of-change in inlet temperature on the compressor system stability margin. The high pressure compressor was more sensitive than the fan to this type of distortion. The main variable affecting stability margin was the magnitude for spatial distortions and the rate-of-change for time-dependent distortions.

Introduction

A recurring problem in the development of air-breathing engine propulsion systems is the detrimental effect of non-uniform inlet flow conditions on engine performance. Of particular concern is the reduction and/or the complete loss of compressor stall margin resulting from aircraft manuevers, coupling with supersonic inlet diffusers, and the ingestion of hot gases from armament firing or recirculation of exhaust gas from a VTOL-type aircraft. A considerable effort has been and is continuing to be exerted in defining and analyzing the effects of non-uniform engine inlet pressure distributions. Some examples of these effects on both turbojet and turbofan compressor systems are contained in Refs. 1 through 4. A less extensive effort has been devoted to defining the effect of non-uniform engine inlet temperatures. Some examples of the effect of inlet temperature transients on turbojet engine compressors are given in Refs. 5 through 7. Very little information is available on the effects of either steady-state or transient inlet temperatures on the performance of the more complex compressor system of a turbofan engine.

In an effort to increase the knowledge and understanding of the effect of these non-uniform inlet flow conditions, a program is currently being conducted at the NASA Lewis Research Center. Part of this program was concerned with the effect of spatial and time-dependent engine inlet temperature distortions on the performance of an afterburning turbofan engine. A gaseous hydrogen fueled heater was used upstream of the engine to provide the temperature distortions. All tests were performed in an altitude facility with an engine inlet pressure approximately one-third atmospheric.

The purpose of this paper is to present and discuss some of the results obtained from the test program. A description of the hydrogen heater, the engine compressor system and the performance instrumentation is given. Results are presented in the form of fan and high pressure compressor maps, and compressor stall margin as effected by the extent, magnitude, and rate of change of the engine inlet temperature distortion. Several examples of both the temperature profiles at the engine inlet during steady-state and transient operation, and the response of the compressor system to a temperature transient are shown.

Apparatus and Instrumentation

Engine

The engine used for this investigation was a two-spool mixed-flow afterburner equiped turbofan. The compressor system was composed of a two-stage fan and a seven-stage high pressure compressor. Each component was driven by a separate turbine unit and speed matching was achieved by aerodynamic coupling. The fan had fixed geometry stator vanes and no inlet guide vanes. The high pressure compressor had variable inlet guide vanes and stators for the first two stages, which were automatically controlled as a function of rotational speed and inlet temperature.

Temperature Distortion Generator

Temperature distortions were produced at the engine face by using a gaseous hydrogen fueled heater located upstream of the engine inlet bellmouth. A description of the heater and the hydrogen supply system is shown schematically on Figure 1. The engine inlet airflow passed through and was heated in a large diameter duct which was divided into four 90^{o} sectors. Each sector contained an array of five annular and two radial v-gutters as shown by the sample in Figure 1. Hydrogen was distributed through a system of tubing located within the v-gutters and fed from a single supply manifold for each sector. Small holes were drilled in the tubing to inject hydrogen into the v-gutters where it was burned. Five swirl-can pilot burners were located in each sector to provide an ignition source for the main hydrogen flow. Temperature control was obtained by varying the hydrogen flow using a slow response remote operated valve for steady-state operation and a high speed remote operated valve for rapid transients. Each sector had its own control system which allowed operation of from one to four sectors thereby producing

spatial or time-dependent temperatures from 90 to 360° of circumferential extent. The system was designed to produce a spatial temperature rise of 800° and time dependent temperature rises in excess of 8000°/sec over a full 360° circumferential extent. Hydrogen was chosen as the fuel because of its good ignition characteristics and rapid flame propagation speed.

Instrumentation

A sketch describing the type, number and location of instrumentation installed in the compression system is presented in Figure 2. Two types of rakes were used at the fan inlet station (2). During spatial temperature distortion testing, the sensing elements at each location were shielded, combined total pressure and total temperature probes. For time-dependent testing, fast response bare-wire chromel-alumel thermocouples were used at each sensing point. These thermocouples were fabricated using 0.003 in. diameter wire and had a computed time constant of 0.013. The thermocouples were designed in accordance with the guidelines set forth in Ref. 8. A total of sixty data sensing points (12 rakes × 5 elements/rake) were sampled at the fan inlet for both steady-state and transient testing. In addition, to the data sensors, each rake contained two thermocouples which were averaged and displayed in the control room for setting the desired temperature level in each sector. No fast response thermocouples were available at the internal instrumentation stations (2.2, 3 and 4). High response total and static pressures were measured at all four instrumentation stations. These measurements were made using miniature strain gage transducers similar to those described in Ref. 9. All steady-state pressure data were measured on a digital automatic multiple pressure recording system (DAMPR). Voltage type signals (transducers, frequency, etc.) were digitized before being recorded. The high response signals were recorded on a high speed digital system (10,000 samples/sec) and on a multiplexed FM analog tape system. The data were reduced in both digital and analog form.

Procedure

Spatial distortion tests. - The desired magnitude and extent of engine inlet temperature was established by regulating the hydrogen flow using the slow acting flow control valves shown in Figure 1. A steady-state data point was recorded and the high speed data systems were activated. Fan stalls were induced by closing down the engine exhaust nozzle area and high pressure compressor stalls were induced by in-flowing high pressure air at the compressor discharge. As soon as a stall was observed, the engine throttle was closed to shut down the engine. The engine was restarted and the desired inlet conditions were re-established. Several steady-state data points were then recorded by either reducing the exhaust nozzle area or increasing the high pressure compressor discharge in-flow air supply to values less than those observed at stall. These steady-state points were then used to estimate the stall point for any given inlet condition.

Time-dependent distortion tests. - The desired engine operating condition was established and steady-state data was recorded. A pressurized volume of hydrogen was "trapped" between the flow control valve and the high speed remote control valves, shown on Figure 1, for the desired number of sectors in the heater. The high speed data systems were activated and the high speed valves were opened using a step input signal. The engine was immediately shut down if stall was observed. The rate-of-change in engine inlet temperature was varied on a trial and error basis by varying the hydrogen pressure in the trapped volumes. The rate-of-change was reduced until a no stall case was obtained for all the circumferential extents tested.

Results and Discussion

Spatial Distortions

Engine inlet conditions. - An example of typical circumferential temperature distributions produced at the engine inlet during testing is shown on Figure 3. These distributions represent the temperatures recorded by the thermocouples located at the middle immersion of each rake at station 2 (see Fig. 2) ratioed to the average temperature at station 2. Both the 360 and 180° extent profiles have additional circumferential gradients imposed upon the desired distribution. An example of the radial temperature gradient that was obtained at the measuring station is shown on the 90° extent profile. This radial gradient was present regardless of the circumferential extent (90, 180, and 360°) but is shown on the 90° extent only for the sake of clarity on the figure. The gradients were the result of non-uniform hydrogen distribution in the heater and varied directly with the magnitude of the temperature being set; i.e., they increased with increasing levels of temperature being generated. The effect of these gradients on the results obtained will be discussed subsequently.

Effect of stability margin. - The effect of the magnitude and circumferential extent of spatial inlet temperature distortions on the stall limits of the fan and high pressure compressor is shown on Figures 4 and 5. The ΔT's referred to on the figures represent the average difference between the heated and non-heated portion of the inlet flow for the 90° and 180° extents and average difference between the engine inlet temperature and the temperature of the air entering the hydrogen heater for the 360° extent.

Comparing the stall points obtained with temperature distortion and the undistorted (clean) inlet fan stall line (Fig. 4) indicates that for ΔT values up to 70° (unheated air at 440° R) the stall line was unaffected by magnitude and extent of circumferential distortion. At values in excess of 70° (for the 90 and 180° extents) the stall points imply that a reduction in stall margin was obtained. However, analysis of the high response pressure instrumentation in the compressor system indicated that the high pressure compressor was the governing component for the stall points obtained at ΔT's in excess of 70°. This is pointed out more clearly on Figure 5 where stall points are shown to occur very near or on the nom-

inal operating line of the core compressor for the high ΔT's and circumferential extents of 90 and 180°. The effect of temperature distortion on the high pressure compressor performance shown on Figure 5 indicates that this component is sensitive to both magnitude and extent of the distortion. This effect is shown on Figure 6 where the percent loss in high pressure compressor stall margin is plotted as a function of the temperature difference between the heated and non-heated engine inlet flow. The percent loss in high pressure compressor stall margin is defined as

$$\% \text{ SM} = \frac{\text{SM}_{\text{distorted}}}{\text{SM}_{\text{undistorted}}} \times 100 \qquad (1)$$

$$\text{SM} = \frac{\text{PR}_{\text{stall}}}{\text{PR}_{\text{O.L.}}} - 1 \left(\text{at constant } \frac{\omega\sqrt{\theta}}{\delta}\right) \qquad (2)$$

These data indicate that all three of the circumferential extents investigated had an effect on the stall margin of the high pressure compressor. The loss in stall margin appears to be only a function of magnitude for both the 90 and 180° extents since the percent in stall margin loss is basically the same. Extent becomes the governing factor when comparing the 360° with the 90 and 180° extents as would be expected. These data also indicated that the loss in stall margin was insensitive to fan rotor speed for the two speeds that were run.

From these results, it appears that the circumferential and radial gradients in the desired inlet temperature distribution had little or no effect on the fan performance. However, the loss in stall margin of the core compressor with the 360° extent indicates that these gradients may have had a slight effect on the high pressure compressor. This effect is basically small, however, when comparing the results to the circumferentially distorted patterns (90° and 180° extents) as shown on Figure 6.

Component interaction. - An example of the interaction between the fan and the high pressure compressor is illustrated in terms of circumferential temperature and pressure profiles on Figures 7 and 8. Since the stability margin investigation indicated that the high pressure compressor was more sensitive to the temperature distortions, the temperature profiles shown for the fan inlet are the local value near the hub ratioed to the average of the temperature readings in the hub region. These values were used since they more closely represent the characteristics of the flow which enters the high pressure compressor. The high pressure compressor inlet and discharge profiles are those obtained from mid-passage thermocouples. For all three of the circumferential extents, the profile remains relatively unchanged in terms of circumferential extent as it passes through the compressor system. A slight attenuation in the magnitude of the distortion is realized as it passes through the compressor system and a rotation in the angular location of the distortion can be observed. The lesser amount of instrumentation at the high pressure compressor inlet and discharge (Fig. 2) did not allow a completely accurate determination of the profiles at these stations.

The resultant high pressure compressor inlet pressure profiles obtained from these temperature distortions are shown on Figure 8. No pressure profiles are shown for the fan inlet and high pressure compressor discharge, since these pressure profiles remained basically the same whether the inlet temperature was distorted or undistorted. These profiles show that a pressure distortion is produced as the flow passes through the fan. The extent and magnitude of the pressure distortion is directly related to the extent and magnitude of the fan inlet temperature distortion. These profiles point out that the high pressure compressor must operate in the presence of both a pressure and temperature distortion even though only a temperature distortion is imposed at the engine inlet.

As an assessment of the cause and effect of these profiles on the stability margin of the two components (fan and high pressure compressor), the circumferential variations in temperature and pressure can be translated into local circumferential variations in component corrected speed and pressure ratio. The results of this approach for a typical 180° circumferential extent engine inlet temperature distortion is shown on the nominal pressure ratio versus corrected speed maps of the two components on Figure 9. The variation in the local (as a function of angular location) experimental pressure ratio of the fan with the calculated local values of corrected speed (based on the experimental inlet temperature profile) shows that the local circumferential operating points agree closely with the undistorted nominal operating line (Fig. 9(a)). This indicates that the magnitude of the pressure distortion at the core compressor inlet can be related to the local reduction in corrected speed of the fan that resulted from the increase in inlet temperature in the distorted region. The local circumferential variation of pressure ratio with local corrected speed of the high pressure compressor did not follow the nominal undistorted operating line (Fig. 9(b)). The compressor was operating at an almost constant local pressure ratio circumferentially even though a variance in computed local corrected speed was obtained based on the circumferential distribution in the high pressure compressor inlet temperature. This characteristic of operation of the two components points out the most probable reason for the core compressor (local operation approaching the undistorted stall line) being the most sensitive to circumferential inlet temperature distortions for this particular compression system. It also points out that temperature distortion (reducing the local corrected speed) was the predominant effect in causing high pressure compressor stall and that the pressure distortion (created by the fan) appears to have had only a secondary effect, if any.

Comparison of pressure and temperature distortions. - A comparison of circumferential temperature and pressure profiles resulting from a screen induced pressure distortion and a hydrogen heater temperature distortion of comparable distortion levels (local/average)

is shown on Figure 10. For both of these conditions the high pressure compressor had a comparable percent loss in stall margin as defined by the previously presented (eq. (1)). The conditions that exist at the high pressure compressor inlet show that a small temperature distortion is produced by the fan when operating with an inlet pressure distortion. However, the predominant effect is the pressure distortion. These comparisons point out that for this particular compressor system, the predominant effect on the high pressure compressor stall margin was directly relatable to the type of engine inlet input distortion; i.e., pressure for a pressure distortion and temperature for a temperature distortion. However, this would not be necessarily true in all cases. For example, in a fan that is designed to provide a significant attenuation of inlet distortions, the secondary effects could become more important than they were for this particular compressor system.

Time-Dependent Distortions

Engine inlet conditions. - Time-dependent temperature distortions were imposed at the engine inlet by the method described in the Procedure section of this paper. Typical examples of the rate-of-change in inlet temperature with time are shown on Figure 11. These curves represent the temperature transient that was realized by the mid-thermocouple in line with one 90^{o} sector of the hydrogen heater. The three curves represent the range of conditions that could be produced by the hydrogen heater. Both the indicated temperature rise (actual thermocouple reading) and the corrected temperature rise are shown in the figure. The designated rate-of-changes represent the maximum slope of the curves during the rise in temperature. The indicated temperatures were corrected for radiation, recovery and time lag using the procedures and equations established in Ref. 8. Because of the significant differences between indicated and corrected values, all subsequent figures and discussion will refer to corrected values only.

During all attempts at producing a 360^{o} time-dependent distortion, spatial distortions were also realized. Typical examples of these characteristics are shown on Figures 12 and 13. The curves shown on Figure 12 represent the corrected temperature rise obtained at the mid-location of all four sectors during a 360^{o} extent transient. Two distinct distortions are shown on this figure; first, the rate-of-change in temperature was not consistent circumferentially and second, a circumferential spatial distortion was obtained at any one instant in time. In addition to these circumferential variations, radial variations were also realized during transients as shown on Figure 13. These radial temperature variations were measured at an angular location (θ^{*}) of 45^{o} and are from the same transient run that is presented on Figure 12. As in the circumferential var-variations both a rate-of-change difference and an instantaneous spatial distortion were obtained.

These circumferential and radial variations are combined into a contour plot as shown on Figure 14. This plot is a representation of the absolute corrected temperatures realized at the engine inlet measuring station approximately 5 milliseconds prior to observing engine stall. The most significant aspect of this flow characteristic at the engine inlet, is that the hottest and most rapidly changing temperatures were concentrated in the hub region of the fan and this is the portion of the flow that entered the high pressure compressor. This same trend was noted during transients run with 90 and 180^{o} extents also and is the most probable reason for the high pressure compressor being the most sensitive to stall during transient temperature ramps. Since these type of temperature profiles were a function of the hydrogen heater design, it was not possible to vary them during this particular experiment and therefore it was not possible to determine if the fan would also have been stall sensitive if the spatial and rate-of-change variations were eliminated.

Compressor system response. - A typical example of the response of the compressor system to a 360^{o} extent engine inlet temperature transient is shown on Figure 15. The lower portion of this figure shows the corrected engine inlet temperatures that were obtained at four angular locations as a function of time. The upper portion shows the time history of pressure at the fan discharge, and high pressure compressor inlet and discharge as recorded by high response pressure instrumentation. Flow breakdown at the high pressure compressor discharge was initiated approximately 30 milliseconds after the inlet temperature began to rise for this test point. A slight reaction at the fan discharge and high pressure compressor inlet can be observed just prior to and during the flow breakdown at the high pressure compressor discharge. Breakdown at the fan discharge lagged the high pressure compressor discharge indicating that the stall propagated forward through the compressor system. This history of events was very typical to that observed during most stalls encountered during transient testing.

Engine stall limits. - The effect of time dependent temperature transients on the engines' stall limit is summarized on Figure 15. For the three circumferential extents tested (90, 180 and 360^{o}), no significant difference was obtained in the rate-of-change in inlet temperature required to produce engine stall. All of the values given for the rate-of-change in temperature are average values obtained from those thermocouples exposed to the temperature transient, i.e. 60 for the 360^{o} extent, 30 for the 180^{o} extent, and 15 for the 90^{o} circumferential extent. It is obvious that locally higher and lower rates were obtained as indicated by the foregoing figures describing the radial and circumferential temperature variations. Therefore the level of the rate of temperature increase required to produce engine stall may not be rigorously accurate however it does indicate that the rate-of-change was more significant than circumferential extent. The difference in absolute temperature (ΔT) obtained at the stall point is also shown on Figure 15. An almost constant level ($\Delta T \approx 50^{o}$) was obtained at the stall points. However, this value is directly related to the rate-of-change in temperature because of the system used to produce the transients. Therefore, no

distinct differentation between rate-of-change and temperature level (ΔT) was obtained, but the temperature levels associated with stall were significantly less than those required to stall the high pressure compressor on its' operating line for steady state spatial distortions (Fig. 5). This indicates that ΔT was a secondary effect on stall for transient testing.

Conclusions

The results of testing a two-spool turbofan engine with both spatial and time-dependent temperature distortions produced by a hydrogen heater, yielded the following principal conclusions concerning the response of the compressor system.

1. The high pressure compressor was the most sensitive component to both spatial and time-dependent temperature distortions.

2. The loss in high pressure compressor stall margin was found to be more dependent upon magnitude rather than circumferential extent for engine inlet spatial temperature distortions.

3. For time-dependent temperature distortions, the rate-of-change in engine inlet temperature had a more pronounced effect than did either circumferential extent or absolute level of temperature obtained during a transient.

4. No determinable reduction in the stall margin of the fan was obtained up to intermediate values of spatial temperature distortion. The fan stall limits were not established at the high values of spatial temperature distortion because core compressor stalls were obtained prior to obtaining fan stalls.

5. A possible explanation of why the core compressor was more sensitive to time dependent temperature distortions may be related to the characteristics of the hydrogen heater profiles produced during transients.

6. The hydrogen heater profiles imposed on the desired circumferential distortions produced during spatial distortion testing appeared to have only a minor effect on the results.

7. The results of this experiment are directly related to this particular compressor system design. A fan of different design may be more sensitive to this type of distortion than was the fan on this particular engine.

Symbols

N rotational speed, rpm

O.L. operating line

P pressure, psia

PR pressure ratio

δ ratio of total pressure to absolute pressure of NACA standard sea-level conditions

S.L. stall line

SM stall margin

T total temperature, ^{o}R

Wa air flow rate, lbs/sec

Δ difference

θ ratio of total temperature to absolute temperature of NACA standard sea-level conditions

θ^* angular location, degrees

Subscripts:

Ave. average

f fan

hpc high pressure compressor

L local

r rated

s static

t total

2 engine inlet

2.2 fan discharge

3 high pressure compressor inlet

4 high pressure compressor discharge

References

1. Alford, J. S., "Inlet Flow Distortion Index," Journées Internationalees de Sciences Aéronautiques, ONERA, Paris, France, May 27-29, 1957, pp. 71-94.

2. Harry, D. P., III and Lubick, R. J., "Inlet-Air Distortion Effects on Stall, Surge, and Acceleration Margin of a Turbojet Engine Equipped with Variable Compressor Inlet Guide Vanes," RM E54K26, 1955, NACA, Cleveland, Ohio.

3. Winslow, L. J., Wendland, D. W., Smith, B. D., and Welliver, A. D., "Inlet Distortion Investigation, Upstream Engine Influence and Screen Simulation," AFAPL-TR-68-140, AD-847095, Jan. 1969, Boeing Co., Seattle, Wash.

4. Werner, R. A., Abdelwahab, M., and Braithwaite, W. M., "Performance and Stall Limits of an Afterburner-Equipped Turbofan Engine with and without Inlet Flow Distortion," TM X-1947, 1970, NASA, Cleveland, Ohio.

5. Wallner, L. E., Useller, J. W., and Saari, M. J., "A Study of Temperature Transients at the Inlet of a Turbojet Engine," RM E57C22, 1957, NACA, Cleveland, Ohio.

6. Childs, J. H., Kochendorfer, F. D., Lubick, R. J., and Friedman, R., "Stall and Flame-Out Resulting from Firing of Armament," RM E55E25, 1955, NACA, Cleveland, Ohio

7. Gabriel, D. S., Wallner, L. E., and Lubick, R. J., "Some Effects of Transients in Inlet Pressure and Temperature on Turbojet Engines," Preprint 709, Jan. 1957, IAS, New York, N.Y.

8. Glawe, G. E., Simmons, F. S., and Stickney, T. M., "Radiation and Recovery Corrections and Time Constants of Several Chromel-Alumel Thermocouple Probes in High-Temperature, High-Velocity Gas Streams," TN 3766, 1956, NACA, Cleveland, Ohio.

9. Armentrout, E. C., "Development of a High-Frequency-Response Pressure-Sensing Rake for Turbofan Engine Tests," TM X-1959, 1970, NASA, Cleveland, Ohio.

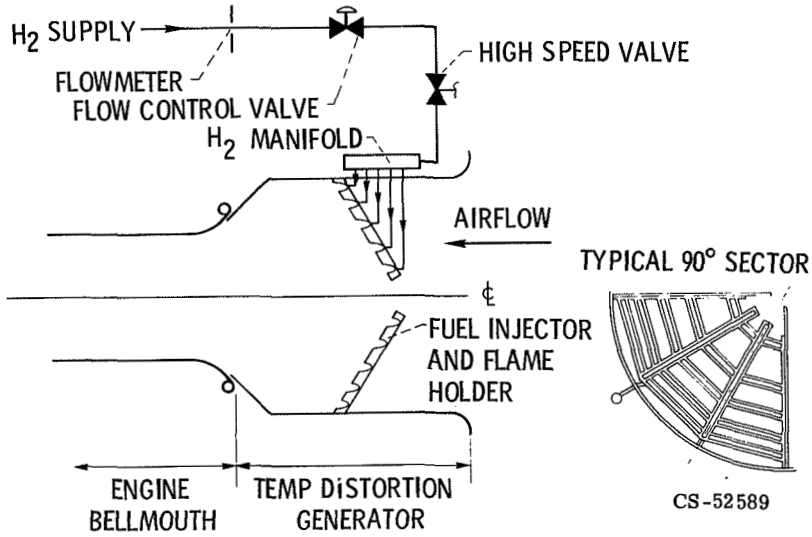

Figure 1. - Hydrogen fueled temperature distortion generator.

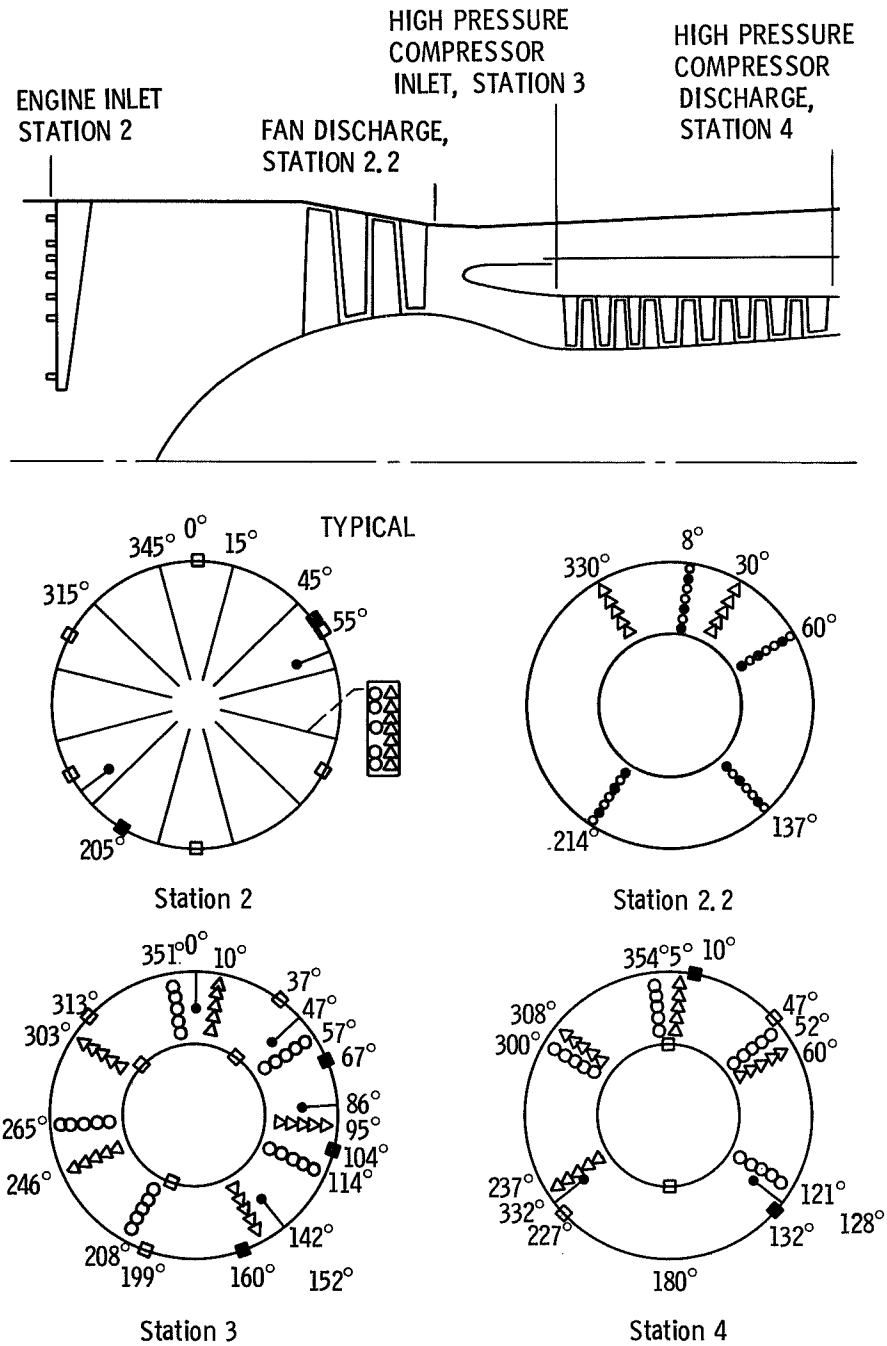

(VIEWED UPSTREAM) ○ = P_t, □ = P_S, △ = T, SHADED SYMBOL = HIGH RESPONSE

Figure 2. - Description of compressor system and instrumentation locations.

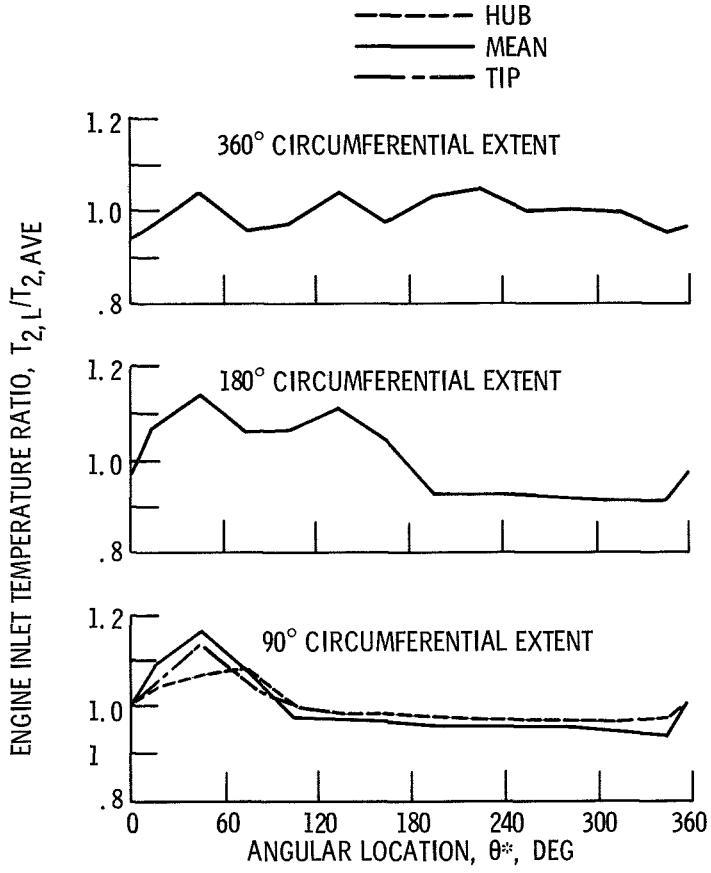

Figure 3. - Typical temperature profiles at engine inlet for spatial temperature distortions.

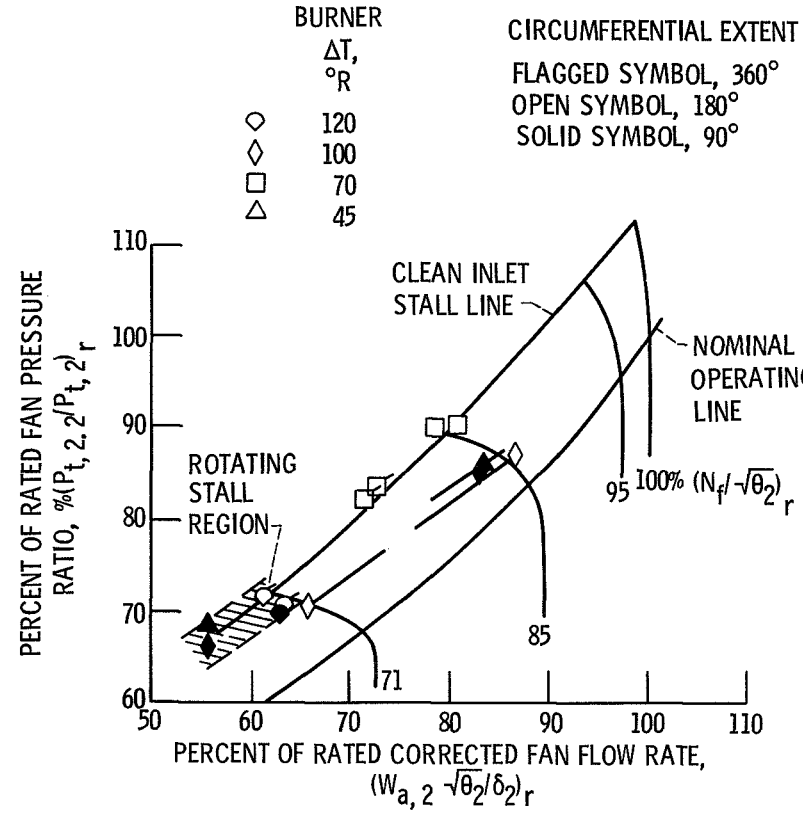

Figure 4. - Effect of spatial temperature distortion on fan stall limits.

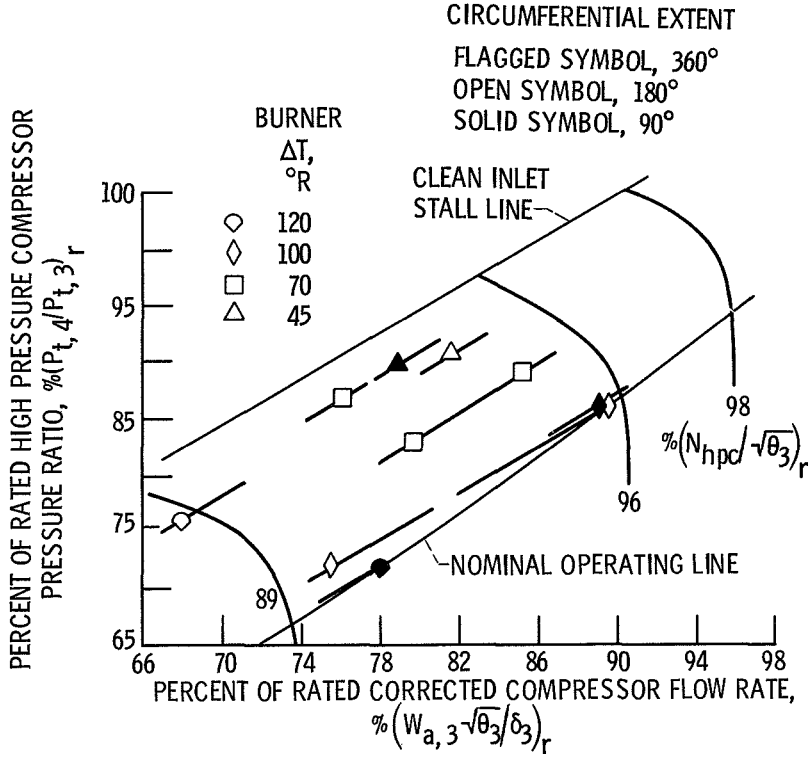

Figure 5. - Effect of spatial temperature distortions on high pressure compressor stall limits.

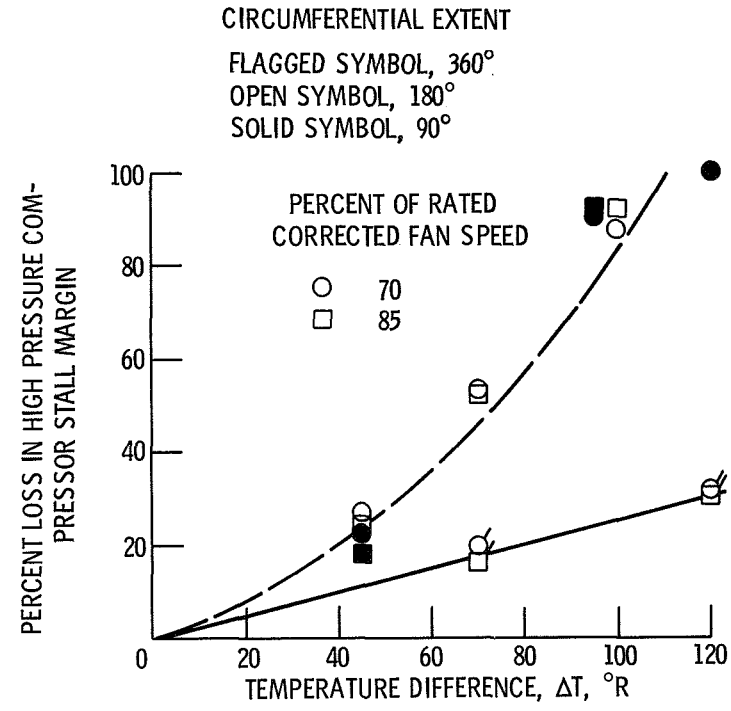

Figure 6. - Loss in high pressure compressor stall margin resulting from spatial temperature distortions.

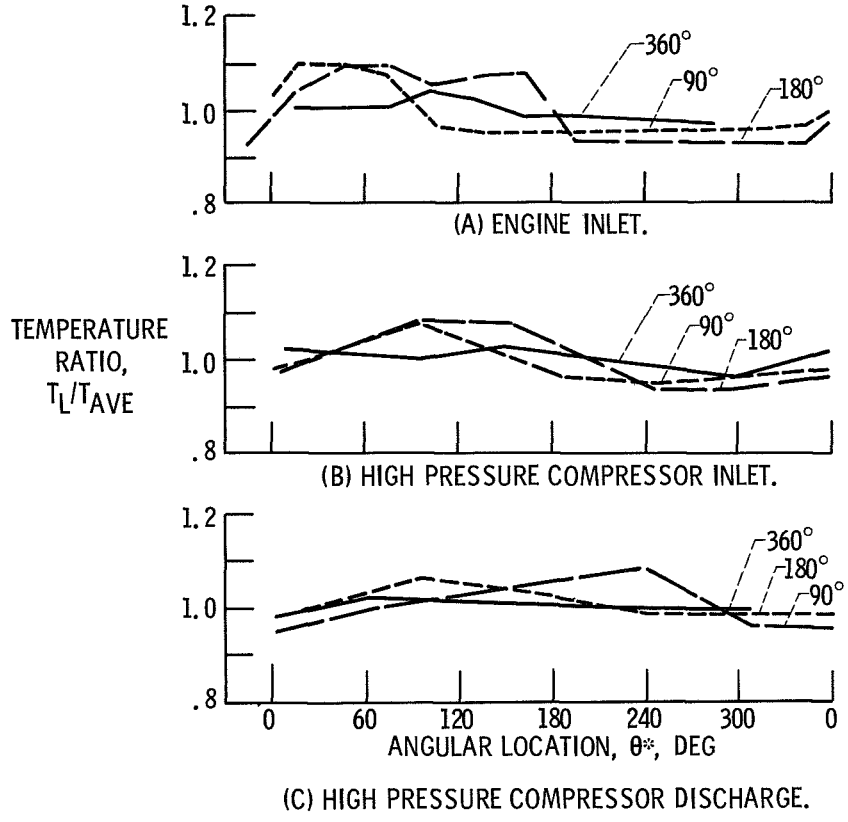

Figure 7. - Temperature profiles through compressor system for spatial temperature distortions.

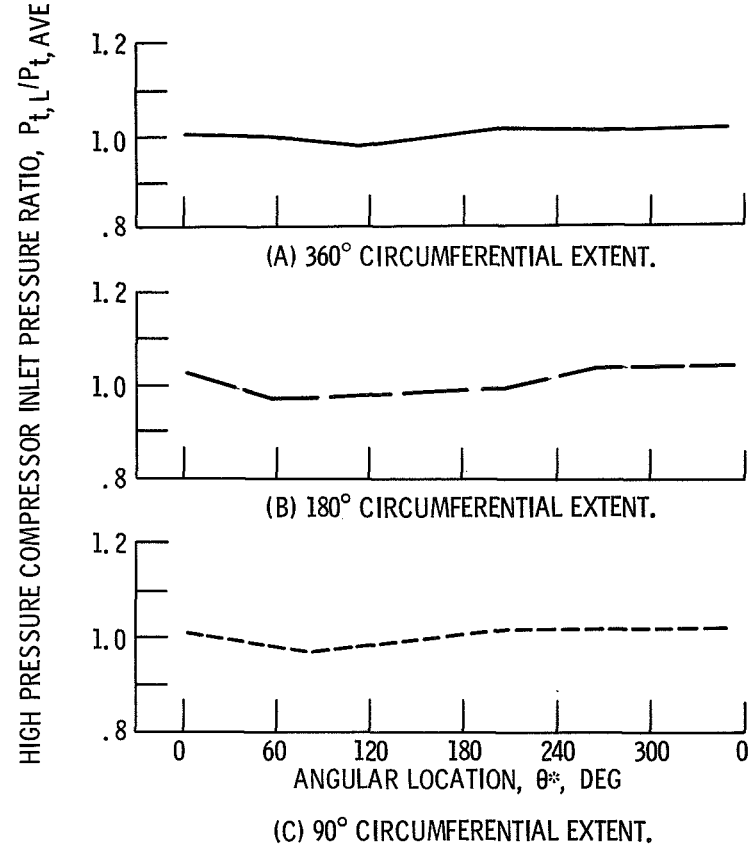

Figure 8. - Pressure profiles at the high pressure compressor inlet generated by a fan inlet temperature distortion.

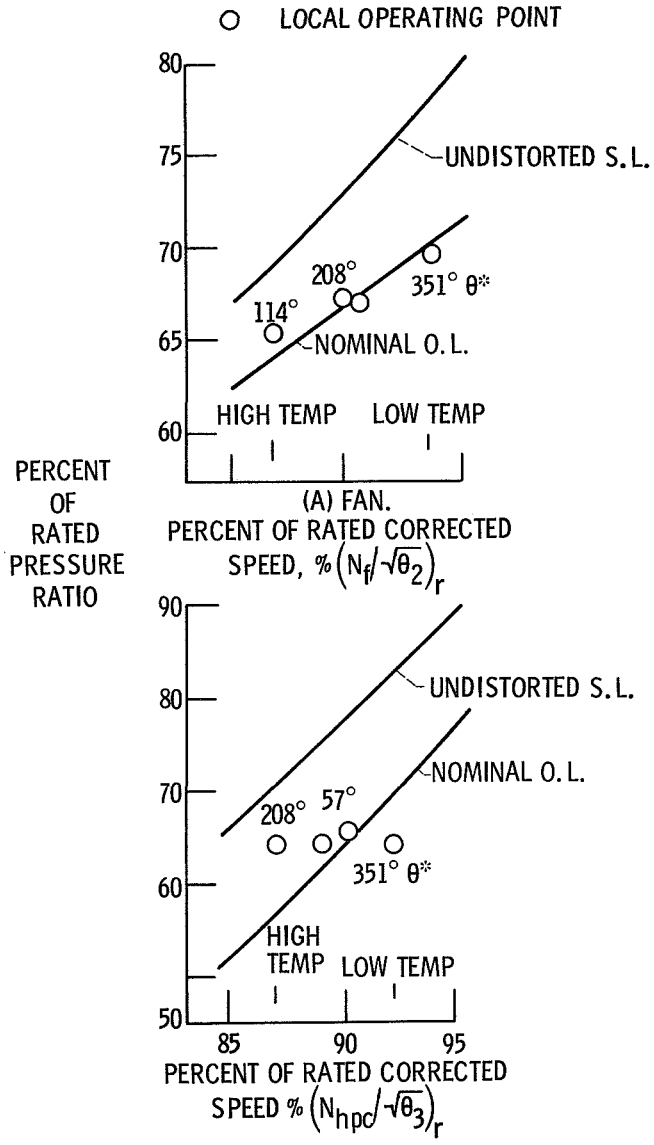

(B) HIGH PRESSURE COMPRESSOR.

Figure 9. - Typical shift in component local operating points; 180° extent spatial temperature distortion.

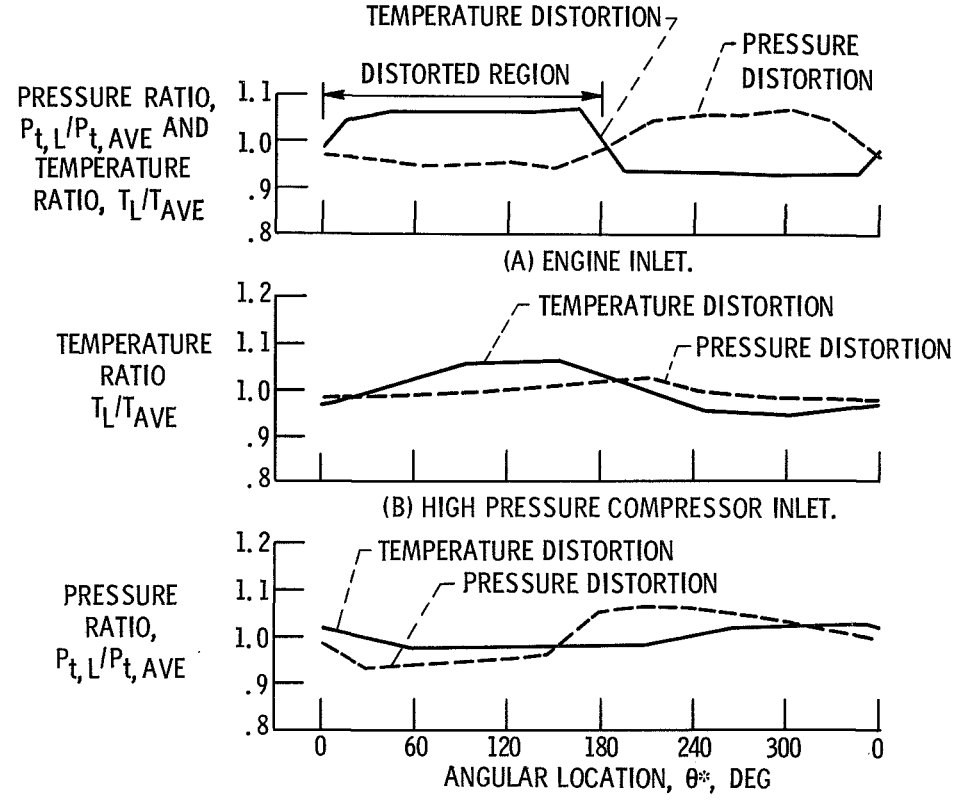

(C) HIGH PRESSURE COMPRESSOR INLET.

Figure 10. - Profile comparisons for pressure and temperature distortions.

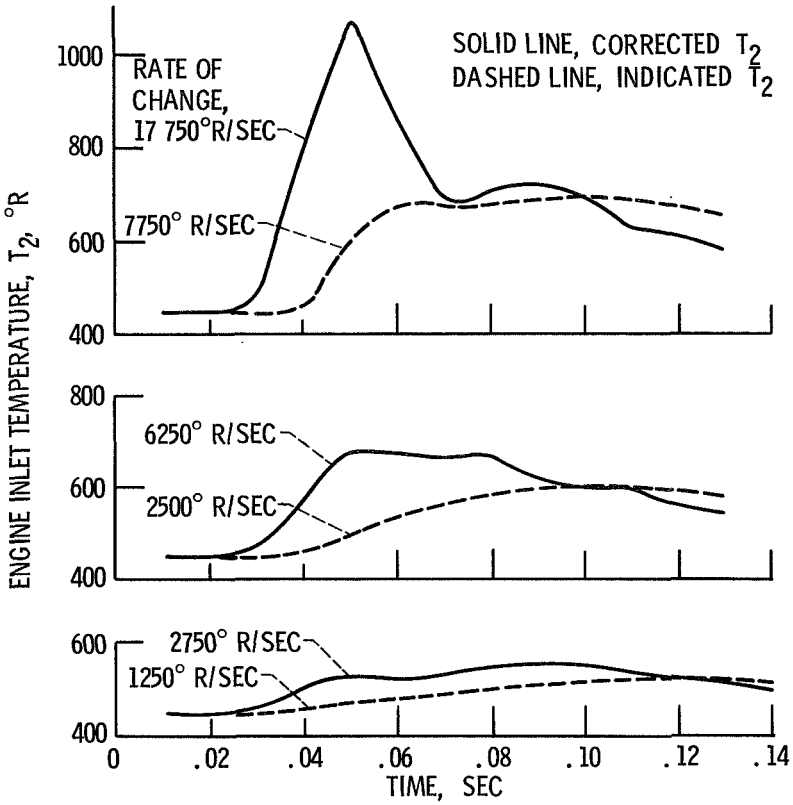

Figure 11. - Typical engine inlet temperature transients.

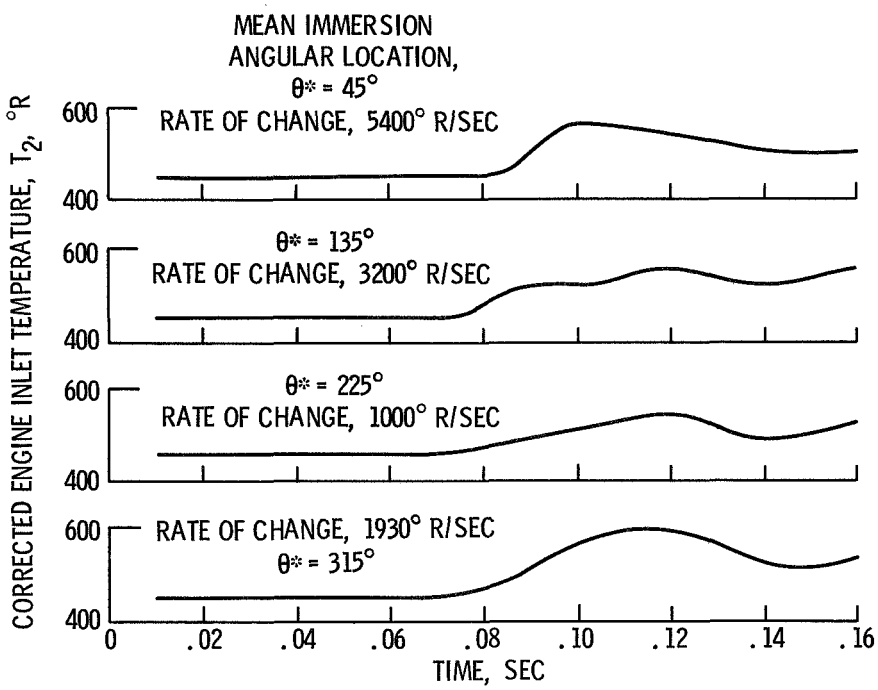

Figure 12. - Circumferential variation in temperature during a 360° extent transient.

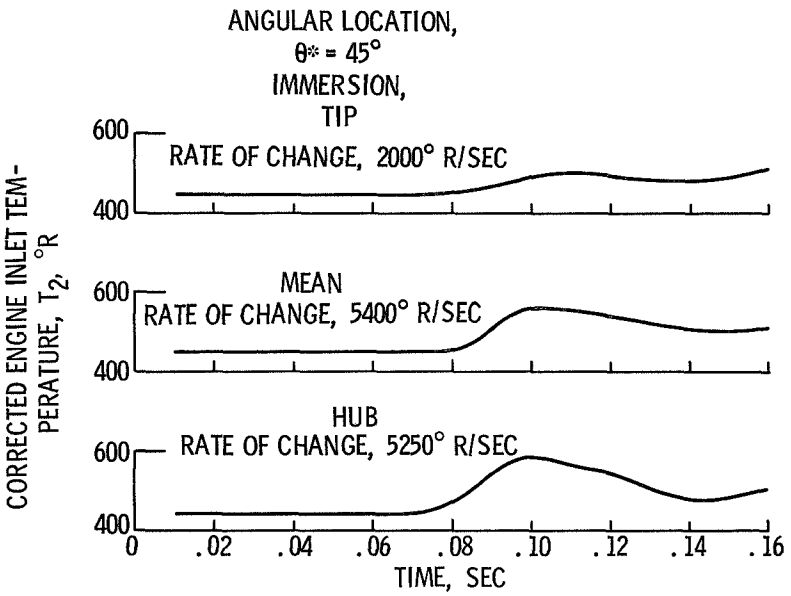

Figure 13. - Radial variation in temperature during a transient.

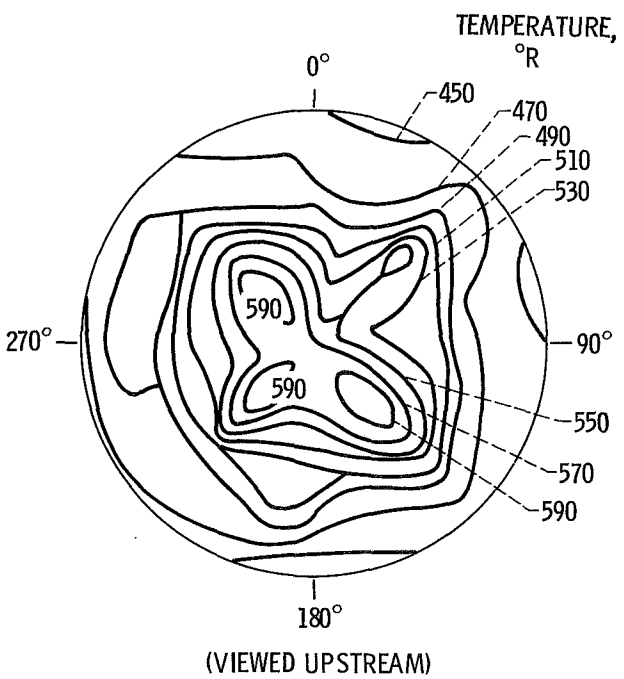

Figure 14. - Instantaneous temperature profiles during a 360° transient just prior to engine stall, temperatures in °R.

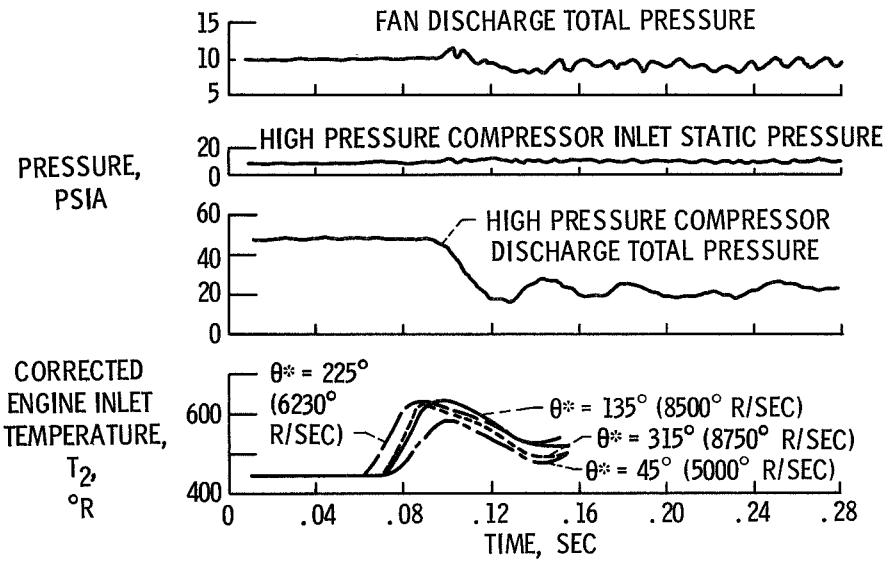

Figure 15. - Response of compressor system to a 360° extent temperature transient.

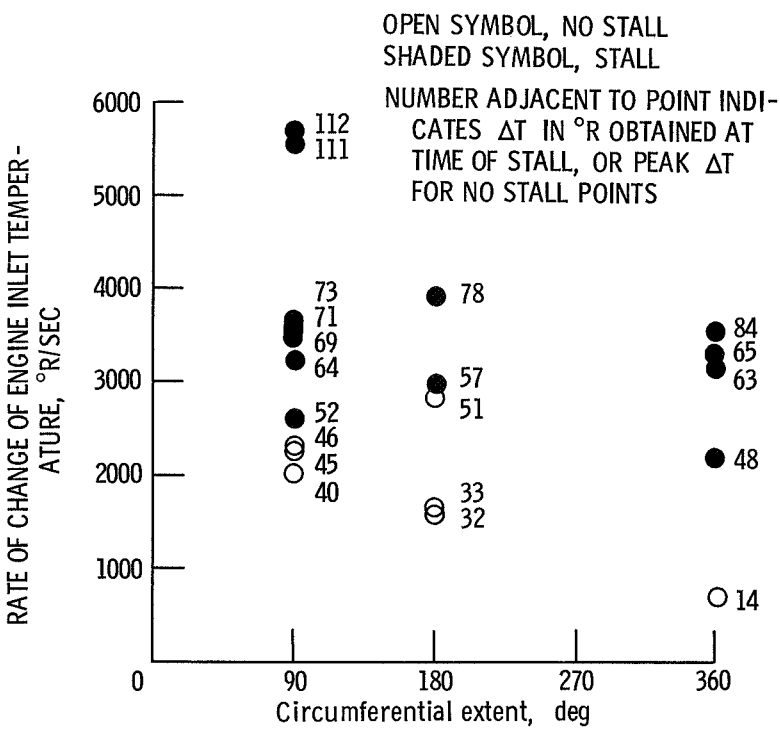

Figure 16. - Effect of time-dependent temperature distortions on engine stall limits.